Since January 2020 Elsevier has created a COVID-19 resource centre with free information in English and Mandarin on the novel coronavirus COVID-19. The COVID-19 resource centre is hosted on Elsevier Connect, the company's public news and information website.

Journal of Clinical Virology 145 (2021) 105019

Contents lists available at ScienceDirect

Journal of Clinical Virology

journal homepage: www.elsevier.com/locate/jcv

CRISPR-cas13 enzymology rapidly detects SARS-CoV-2 fragments in a clinical setting

Wahab A. Khan [a,b,*], Rachael E. Barney [b], Gregory J. Tsongalis [a,b]

[a] Department of Pathology and Laboratory Medicine, The Audrey and Theodore Geisel School of Medicine at Dartmouth College, Hanover, NH 03755, United States of America

[b] Laboratory for Clinical Genomics and Advanced Technology, Department of Pathology and Laboratory Medicine, Dartmouth Hitchcock Medical Center, 1 Medical Center Drive, Lebanon, NH 03756, United States of America

ARTICLE INFO

Keywords:
SARS-CoV-2
CRISPR technology
RT-Lamp
Cas13 enzymology
Fluorescence readout

ABSTRACT

Background: The well-recognized genome editing ability of the CRISPR-Cas system has triggered significant advances in CRISPR diagnostics. This has prompted an interest in developing new biosensing applications for nucleic acid detection. Recently, such applications have been engineered for detection of SARS-CoV-2. Increased demand for testing and consumables of RT-PCR assays has led to the use of alternate testing options. Here we evaluate the accuracy and performance of a novel fluorescence-based assay that received EUA authorization for detecting SARS-CoV-2 in clinical samples.

Methods: The Specific High-Sensitivity Enzymatic Reporter UnLOCKing (SHERLOCK) technology forms the basis of the Sherlock CRISPR SARS-CoV-2 kit using the CRISPR-Cas13a system. Our experimental strategy included selection of COVID-19 patient samples from previously validated RT-PCR assays. Positive samples were selected based on a broad range of cycle thresholds.

Results: A total of 60 COVID-19 patient samples were correctly diagnosed with 100% detection accuracy (relative fluorescence ratios: N gene 95% CI 29.9–43.8, ORF1ab gene 95% CI 30.1–46.3). All controls, including RNase P, showed expected findings. Overall ratios were robustly distinct between positive and negative cases relative to the pre-established 5-fold change in fluorescence.

Conclusions: We have evaluated the accuracy of detecting conserved targets of SARS-CoV-2 across a range of viral loads, including low titers, using SHERLOCK CRISPR collateral detection in a clinical setting. These findings demonstrate encouraging results, at a time when COVID-19 clinical diagnosis and screening protocols remain in demand; especially as new variants emerge and vaccine mandates evolve. This approach highlights new thinking in infectious disease identification and can be expanded to measure nucleic acids in other clinical isolates.

1. Background

The novel infectious severe acute respiratory syndrome coronavirus 2 (SARS-Cov-2) emerged in Wuhan, China in late 2019 and has since become a global pandemic[1]. From reports of the initial set of infected patients[2–4], emerging evidence continues to reflect that some individuals experienced severe conditions requiring intensive care and hospitalization with a significant number succumbing to the virus. In the majority of patients, the clinical course typically ranged from marked fever, myalgia, pneumonia to dyspnea and respiratory distress[2–4]. As we learned more about the disease course, it became apparent that most individuals present with mild symptoms, but more importantly, asymptomatic or low-level infected individuals can become carriers who further potentiate the spread of the COVID-19 disease [5,6].

Mitigating the spread of the virus clearly involves accurate, efficient and increased testing with a simultaneous public health surveillance and screening efforts. The gold standard test uses quantitative reverse transcriptase polymerase chain reaction (RT-PCR) approach. RT-PCR based approaches for SARS-CoV-2 typically require detection of multiple targets. For this, several pre-requisites need to be in place such as having hydrolysis sequence-specific probes that need to be labeled with a distinct fluorescent dye and an appropriate quencher moiety. The emission maxima of the dyes must not overlap with each other and reactions need to be carried out on an appropriate real-time cycler that

* Corresponding author.
E-mail address: wahab.a.khan@hitchcock.org (W.A. Khan).

https://doi.org/10.1016/j.jcv.2021.105019
Received 1 February 2021; Received in revised form 27 July 2021; Accepted 19 October 2021
Available online 28 October 2021

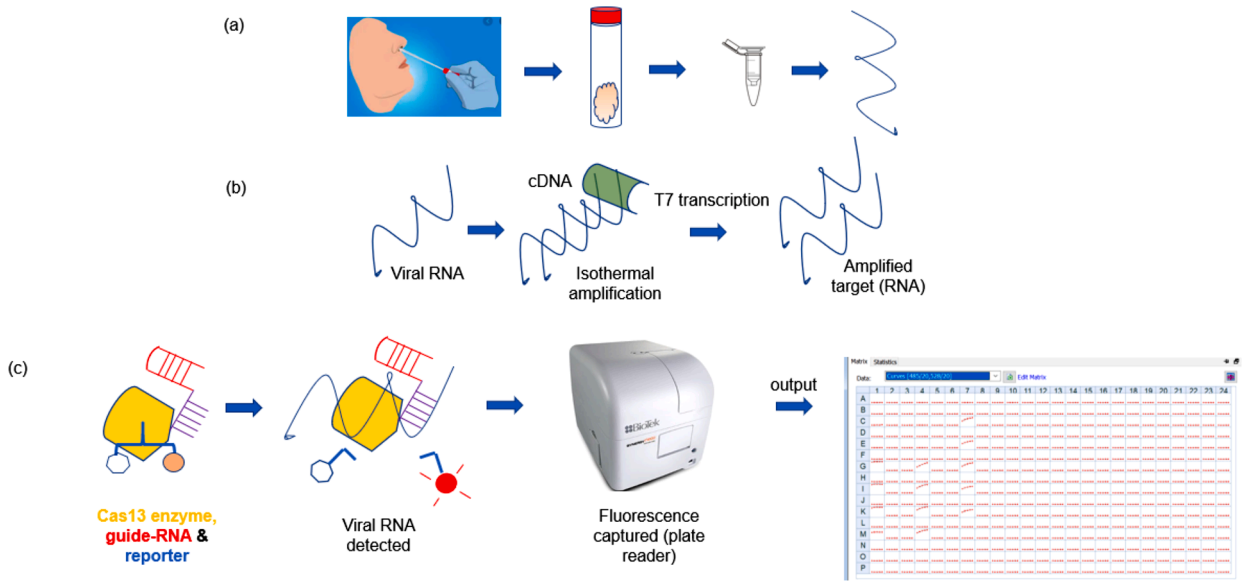

Fig. 1. Basic workflow of CRISPR-Cas13 detection of SARS-CoV-2 as it relates to pre-processing, analytical and post-analytical steps. (a) Upon collection of nasopharyngeal swab and nucleic acid extraction, the purified RNA is subjected to an (b) isothermal amplification (green depicts the reverse transcriptase enzyme). (c) The amplified target upon being bound by the Cas13 enzyme (yellow), with its guide RNA (purple-red) cleaves the reporter (blue). A standard output generated on a plate reader is shown form which data export using a macro language function is performed. All sequence of events are shown in succession left to right in panels a-c.

supports multiplex analysis. Further, for downstream quantification, the efficiency of the method may vary between RT-PCR runs and reactions. Taken together, although PCR is very effective in optimized scenarios, these pre-requisites can limit the use of PCR testing in locations outside central laboratories. Therefore, frequent, rapid, and portable testing is necessary; especially with the already limited resources for RT-PCR based reagents and consumables. This has prompted new strategies for viral RNA detection of SARS-CoV-2. Clustered regularly interspaced short palindromic repeats (CRISPR) can complement RT-PCR testing and provide suitable sensitivity and high specificity. This approach uses guide RNA enzymes from the Cas family (i.e. Cas12, Cas13) that are engineered with a programmable spacer sequence and nucleotide binding domains that can cleave the nucleic acid target of interest[7,8].

In the current study, we employ the Specific High Sensitivity Enzymatic Reporter UnLOCKing (SHERLOCK) technology that was initially described as a means to rapidly detect nuclei acids in human health applications. In particular, this was applied to instances where different strains of the Zika and Dengue viruses as well as other pathogenic bacteria needed to be distinguished [9,10]. It has since been used to identify mutations in cell-free tumor DNA in the background of genomic DNA and has broad applications in genotyping human DNA[9]. The current approach naturally leverages SHERLOCK as a CRISPR-based diagnostic platform to detect SARS-CoV-2 viral RNA. In terms of material cost, the SHERLOCK assay is comparable to RT-PCR and can be further reduced at production scale ($0.60–0.70/reaction)[11]. The CRISPR guide RNA is a short RNA sequence that is cheap to synthesize and the quencher has a fixed sequence that does not need to be redesigned and ordered for each new target[12] Of note, the expense for detection platforms such as a fluorescent plate reader and incubator are also lower than purchasing a RT-PCR instrument[12]. The main principal behind SHERLOCK is that in the presence of SARS-CoV-2 viral RNA, a Cas13 enzyme complexed with a virus targeting RNA will be activated and will cleave the viral RNA resulting in collateral RNase activity[7,12].

The sensitivity and specificity of the assay to detect synthetic SARS-CoV-2 viral RNA was determined by Sherlock Biosciences as part of the emergency use authorization (EUA) and was successfully submitted to the FDA (https://www.fda.gov/medical-devices/coronavirus-covid-19-and-medical-devices/sars-cov-2-reference-panel-comparative-data). Each viral RNA target (Nucleocapsid or N gene, Open Reading Frame 1ab or O gene) was tested in triplicate over a range of 10 dilutions. The estimated limit of detection for the N and O target was determined to be 0.9 and 4.5 copies/μL, respectively, of viral transport media (VTM). The limit of detection was confirmed by testing at 1.5x the estimated limit of detection, which was determined to be 6.75 copies/μL of VTM from 19 out of 20 samples with a 95% detection rate (https://www.fda.gov/media/137747/download). Here we extend this work and present a clinical evaluation of the SHERLOCK approach in a CLIA-certified molecular diagnostics laboratory performing high complexity testing for detection of SARS-CoV-2.

2. Methods

2.1. Overview of experimental protocol

The Sherlock CRISPR SARS-CoV-2 kit has two main parts and was completed in under 2 hr from a brief reverse transcriptase loop-mediated amplification (RT-LAMP)[13] step to direct CRISPR detection of the RNA targets in 10 min. In the first step, SARS-CoV-2 RNA is reverse transcribed to DNA and the DNA is amplified by a strand displacing DNA polymerase. The second step initiates transcription of the DNA and activates collateral cleavage activity of CRISPR complex programmed to the target RNA sequence (i.e. programmable crRNA)[12]. As Cas13 cleaves the reporter RNA molecules, separating the two ends, a fluorescent signal is detected on a standard plate reader (Fig. 1). SHERLOCK technology was designed to detect fragments of the N and the O genes of SARS-CoV-2. A third target, the human RNase P *POP7* (RP) gene, acted as an internal extraction control. Of note, and unlike most molecular assays, SHERLOCK identifies SARS-CoV-2 RNA rather than cDNA providing increased target specificity. In the current experimental protocol, upper respiratory specimens mainly from nasopharyngeal swabs were tested. All experimental procedures were performed under strict cross contamination controls with minimal handling steps in the process. The CRISPR-Cas mix and RT-LAMP process were subjected to multi-channel pipetting. This sufficiently decreased the number of handling steps. We also incorporated the use of aerosol barrier tips, maintained separate dedicated pipettes, employed unidirectional workflow, and used an air clean instrument (i.e. ductless fume hood)

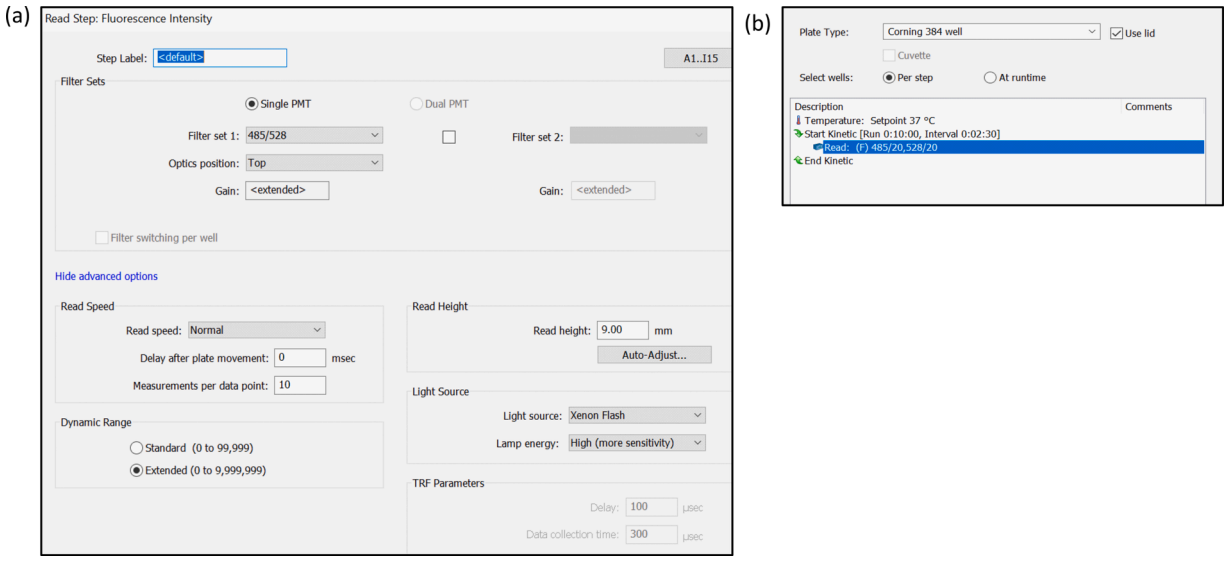

Fig. 2. Settings on BioTek plate reader applied during SARS-CoV-2 detection step. (a) The read speed was set to normal and standard filter excitation and emission spectra were all collected at 485/528 respectively. (b) Settings for collecting data is broken up into 2.5-minute intervals with a total kinetic read time of 10 min.

designed to protect the operator and the process.

2.2. Specimen collection and preparation

All sample collection and preparation steps were performed in accordance with CDC interim guidelines (https://www.cdc.gov/coronavirus/2019-ncov/lab/). The extraction of RNA from nasopharyngeal swabs placed into VTM was carried out using the QIAGEN EZ1 virus mini v 2.0 kit on the EZ1 advanced XL instrument. Samples were eluted in a final volume of 120µL. A total of 8 µL of the extracted RNA was used in a given CRISPR reaction and the remaining stored in aliquots at -80°C for subsequent use. The RT-LAMP master mix (IDT, catalog # 10,006,968) was prepared separately with primer pairs (10x concentrate) targeting the N, O, and the RP gene as an internal quality control step. A no template or NTC control along with a SARS-CoV-2 positive control (BEI; Catalog # NR-52,285) was included in final reaction volumes of 20µL. The latter was diluted to a stock concentration of 4800 copies/µL.

2.3. CRISPR CAS preparation and detection

The Cas master mix reaction with the N, O," and RP specific guide RNAs (crRNA), reporter reagent, and LwaCas13a enzyme was prepared according to manufacturer's instructions (IDT, Sherlock™ CRISPR SARS-CoV-2 kit). This mixture was distributed into separate reaction strip tubes of 20 µL aliquots. To each respective 20 µL Cas13 mix, 5 uL of RT-LAMP reaction containing the test sample and appropriate controls was added and the reaction mixture vortexed for ~10 sec. A final volume of 20 µL of the mixture was transferred, based on a pre-designated layout indicating the spot location of each sample, to a 384-well flat low-volume clear bottom assay plate (Corning, catalog # 3540). This step was performed in an air clean system to avoid cross-contaminants. The plate was protected with a microamp optical adhesive film (Applied Biosystems, catalog # 4,311,971), prior to loading onto a pre-warmed multimode plate reader (BioTek Synergy NEO2). All steps were performed in a unidirectional workflow.

2.4. Data processing and analysis

The specific plate reader configuration settings for initiating the analysis are provided in Fig. 2. Following the 10-minute sample analysis protocol, raw fluorescence data from each well of the assay plate was transferred into an excel document. The raw data were then normalized by dividing target reaction fluorescence accumulated at time point 10 min ($t_{10\ min}$) of the test sample to that of the NTC reaction, also measured at the same time point interval. This generated a quantitative result in the form of a ratio. Briefly a result was considered "detected" or positive if *either* SARS-CoV-2 target (i.e. N or O) reaction produced a fluorescence ratio that was greater than or equal to a 5-fold increase in florescence measured at 10 min for the test sample over the corresponding NTC reaction control. And if this ratio calculated as less than a 5-fold increase in reaction fluorescence for *both* SARS-CoV-2 targets (either N or O), the result was considered as "not detected" or negative. It should be noted that a result is invalid if all targets (N, O, RP) exhibited less than 5-fold increase in reaction fluorescence. Additional specifics to the ratio calculation and interpretative outputs are tabulated in Table 1.

Table 1
List of ratio combinations and interpretation for reporting SARS-CoV-2 results on clinical samples. Three targets are listed, including the RNAse P *POP7* gene which serves as a control for the extraction of the clinical sample in the absence of a positive SARS-CoV-2 result. Note the experiment should also be considered invalid if the NTC (not shown in table) shows a ratio >5.

N	ORF1ab	RNase P	Interpretation
≥ 5	≥ 5	n/a	Detected
≥ 5	≤ 5	n/a	Detected
≤ 5	≥ 5	n/a	Detected
≤ 5	≤ 5	≥ 5	Not Detected
≤ 5	≤ 5	≤ 5	Invalid

3. Results

3.1. Clinical specimen testing

For our SHERLOCK experimental design, we utilized de-identified clinical patient samples previously tested using the SARS-CoV-2 CDC assay on the Applied Biosystems 7500Fast Dx instrument implemented near the start of the pandemic by our molecular laboratory [14]. These patient results were also subsequently confirmed using orthogonal technologies from Abbott (m2000 real-time system) and ChromaCode (HDPCR™ SARS-CoV-2 real-time PCR assay). Samples within three categories of cycle threshold (Ct) values (low positive: 30–36; mid positive: 15–30; high positive: 5–15) were included in the analysis,

Table 2
Summary of clinical SARS-CoV-2 nasopharyngeal samples processed on the SHERLOCK CRISPR-Cas13 assay with comparable concordance to the RT-PCR CDC (Ct cut off for detection = 41.5) and chromacode HDPCR SARS-CoV-2. * Indicates pooled set of samples processed on Abbott's M2000rt platform. Note; some of the highest reported Ct values (weak positives**) from the CDC and chromacode assays were tested with the SHERLOCK chemistry and showed close concordance with RT-PCR.

Sample	SARS-CoV-2 gene target fluorescence at 10 mins		Extraction control	NTC fluorescence at 10 mins			SHERLOCK assay ratios (>5 = detected & < 5 = not detected)			Ct values from RT-PCR platforms	Concordance
	N	ORF1ab	RNAseP	N	ORF1ab	RNAseP	N	ORF1ab	RNAseP		
1	335,840	257,916	222,233	20,408	7625	10,149	16.46	33.83	21.90	Detected/Ct = 17.44	Y
2	11,112	9133	224,657				0.54	1.20	22.14	Not Detected	Y
3	8055	4966	170,538	7885	4792	6883	1.02	1.04	24.78	Not Detected	Y
4	7982	4490	160,942				1.01	0.94	23.38	Not Detected	Y
5	212,383	162,298	180,997				26.94	33.87	26.30	Detected/Ct = 20.96	Y
6	303,393	230,758	216,275				38.48	48.15	31.42	Detected/Ct = 29.85**	Y
7	387,741	198,326	190,924				49.17	41.39	27.74	Detected/ Ct = 19.52	Y
8	6483	5449	178,434	6976	4942	5961	0.93	1.10	29.93	Not Detected	Y
9*	398,533	236,583	176,738				57.13	47.87	29.65	Detected/Ct = 7.11	Y
10*							57.13	47.87	29.65	Detected/Ct = 6.61	Y
11*							57.13	47.87	29.65	Detected/Ct = 9.72	Y
12	12,762	6152	287,888	9956	7251	6246	1.28	0.85	46.09	Not Detected	Y
13	10,212	6124	266,406				1.03	0.84	42.65	Not Detected	Y
14	332,171	296,684	287,583				33.36	40.92	46.04	Detected/Ct = 27.7	Y
15	338,260	326,265	257,692				33.98	45.00	41.26	Detected/Ct = 33.3**	Y
16	325,267	336,348	227,281				32.67	46.39	36.39	Detected/Ct = 17.7	Y
17	5194	10,836	176,183	5606	3952	5078	0.93	2.74	34.70	Not Detected	Y
18	5662	3582	202,351				1.01	0.91	39.85	Not Detected	Y
19	5036	19,513	186,814				0.90	4.94	36.79	Not Detected	Y
20	5102	3586	189,368				0.91	0.91	37.29	Not Detected	Y
21	7625	4375	178,607	7003	4473	7253	1.09	0.98	24.63	Not Detected	Y
22	246,413	4297	159,377				35.19	0.96	21.97	Detected/Ct = 36.06**	Y
23	335,543	545,207	238,894	8833	4433	7879	37.99	122.99	30.32	Detected/Ct = 33.3**	Y
24	7147	248,867	218,673				0.81	56.14	27.75	Detected/Ct = 32.88**	Y
25	346,489	498,365	340,415				39.23	112.42	43.21	Detected/Ct = 24.05	Y
26	381,772	561,364	315,811				43.22	126.63	40.08	Detected/Ct = 22.42	Y
27	280,690	305,274	305,007				31.78	68.86	38.71	Detected/Ct = 17.52	Y
28	276,274	270,071	315,212				31.28	60.92	40.01	Detected/Ct = 18.1	Y
29	324,165	257,089	225,351	6347	4492	6447	51.07	57.23	34.95	Detected/Ct = 21.9	Y
30	345,856	234,039	186,853				54.49	52.10	28.98	Detected/Ct = 31.8**	Y
31	311,710	244,545	191,391				49.11	54.44	29.69	Detected/Ct = 28.5	Y
32	300,441	239,601	202,344				47.34	53.34	31.39	Detected/Ct = 24.7	Y
33	324,643	207,806	187,956				51.15	46.26	29.15	Detected/Ct = 15.6	Y
34	305,808	244,574	190,052				48.18	54.45	29.48	Detected/Ct = 21.0	Y
35	322,784	274,537	200,890				50.86	61.12	31.16	Detected/Ct = 17	Y
36	306,715	255,320	163,073				48.32	56.84	25.29	Detected/Ct = 27.7	Y
37	325,232	246,979	193,283				51.24	54.98	29.98	Detected/Ct = 21.1	Y
38	325,197	168,880	171,895				51.24	37.60	26.66	Detected/Ct = 23.2	Y
39	317,602	249,112	242,150				50.04	55.46	37.56	Detected/Ct = 30.8**	Y
40	359,819	181,938	193,781				56.69	40.50	30.06	Detected/Ct = 23.3	Y
41	320,959	219,460	234,646				50.57	48.86	36.40	Detected/Ct = 18.6	Y
42	422,682	202,531	163,150				66.60	45.09	25.31	Detected/Ct = 15.1	Y
43	7721	3474	161,671	4791	3097	5088	1.61	1.12	31.77	Not Detected	Y
44	4566	3699	155,285				0.95	1.19	30.52	Not Detected	Y
45	4395	3412	165,760				0.92	1.10	32.58	Not Detected	Y
46	4392	3486	141,616				0.92	1.13	27.83	Not Detected	Y
47	4265	3469	165,297				0.89	1.12	32.49	Not Detected	Y
48	3911	3444	163,259				0.82	1.11	32.09	Not Detected	Y
49	241,836	171,766	170,847				50.48	55.46	33.58	Detected/Ct = 19.5	Y
50	335,201	140,939	179,742				69.96	45.51	35.33	Detected/Ct = 19.9	Y
51	533,800	173,437	191,745				73.17	23.96	35.97	Detected/Ct = 10.84	Y
52	387,490	226,264	144,137	7295	7238	5331	53.12	31.26	27.04	Detected/Ct = 5.21	Y
53	560,698	237,724	4902				76.86	32.84	0.92	Detected/Ct = 7.23	Y
54	663,657	296,031	7003				90.97	40.90	1.31	Detected/Ct = 3.41	Y
55	560,017	188,136	130,854				85.39	49.47	25.68	Detected/Ct = 27.64	Y
56	422,493	389,908	149,072				64.42	102.53	29.25	Detected/Ct = 14.72	Y
57	560,179	377,374	156,198				85.42	99.23	30.65	Detected/Ct = 32.99**	Y
58	456,913	195,350	173,756				69.67	51.37	34.10	Detected/Ct = 16.18	Y
59	410,677	6911	157,596				62.62	1.82	30.93	Detected/Ct = 30.92**	Y
60	436,841	140,768	132,389	6558	3803	5096	66.61	37.01	25.98	Detected/Ct = 19.93	Y

Table 3
Contingency table summarizing RT-PCR results compared to Sherlock SARS-CoV-2 kit detecting positive and negative nasopharyngeal clinical samples (n = 60; N gene 95% CI 29.9–43.8, ORF1ab gene 95% CI 30.1–46.3). The overall concordance, sensitivity, and specificity of all the samples processed compared to the reference method was 100%.

		RT-PCR (Ref. Method)		
		Positive	Negative	Total
SHERLOCK CRISPR (Candidate method)	Positive	43 (TP)	0 (FP)	43
	Negative	0 (FN)	17 (TN)	17
	Total	43	17	60

where the Ct value is inversely proportional to the viral copy number. A total of 43 positive (SARS-CoV-2 detected) and 17 negative samples were analyzed (n = 60 total) using the SHERLOCK Cas13 technology.

3.2. SHERLOCK assay performance

The SHERLOCK assay correctly confirmed all 60 previous clinical sample results (Table 2) with 100% sensitivity and specificity (Table 3). A series of pooled positive samples that were tested in triplicate also showed consistent results and reproducibility of the assay. Clinical sample numbers 22, 24, and 59 were also concordant with the reference method as one of the two targets reported a 5-fold increase in fluorescence measurement at 10 min over the NTC (Table 2). The raw signal output graph on the BioTek Gen5 software clearly demarcated a positive result relative to a negative one with a marked increase in relative fluorescence (Fig. 3). Ratios calculated from the raw fluorescence values at t_{10min} for test samples were nearly 45 to 55-fold higher for the N and O gene targets (ratios > 5) respectively for a positive Cas13 detection relative to a negative finding. This further suggests that the collateral cleavage activity of the CRISPR complex is robust at differentiating infected from non-infected patients in our cohort with high accuracy. All positive, negative, and internal extraction control – RP; performed as expected with normalized fluorescence ratios well below a 3-fold increase cut-off for the NTC (Table 2).

3.3. Potential for scale-up

In terms of sample set-up and processing, we have currently observed optimal detection in a 384-well plate system, given the volumes of the Cas13 detection reaction used as part of the experimental design. This small diameter of the sample vessels in which the CRISPR reactions commence maximally retains fluorescence and promotes favorable molecular collisions during the SHERLOCK step. However, increasing the Cas detection volume may allow for comparable detection using a 96-well format. We can accommodate approximately 200 samples on one plate if every other well in a 384-well column configuration is omitted to pre-emptively minimize any risk for contamination. On a Hamilton STAR system or similar [15], both a 384 and a 96 probe head with rocket tips can potentially process up to 5 plates for an output of approximately 1000 samples in 24 hrs.

4. Discussion

We have successfully demonstrated the diagnostic potential of SHERLOCK CRISPR-Cas13 enzymology for the detection of SARS-CoV-2 in 60 previously tested patient samples. In this proof of principal study, all samples subjected to this approach were in keeping with results reported for detecting SARS-CoV-2. Our false positive/negative rates were low (Table 3) and detection accuracy 100% compared to the gold standard. A major advantage of CRISPR based diagnostics is that it is highly specific, because the Cas13a RNase remains dormant until it binds to its specific programmed RNA target [16]. One limitation of the current work is that it was performed in a smaller subset of COVID-19 clinical samples that were available with a focus towards evaluating sample concordance with RT-PCR. However, given that reagents volumes are amenable to being scaled and guide RNAs cheaply designed; this assay has the potential for higher throughput testing capacity.

CRISPR-Cas13 as well as Cas12 have also shown efficacy in detecting

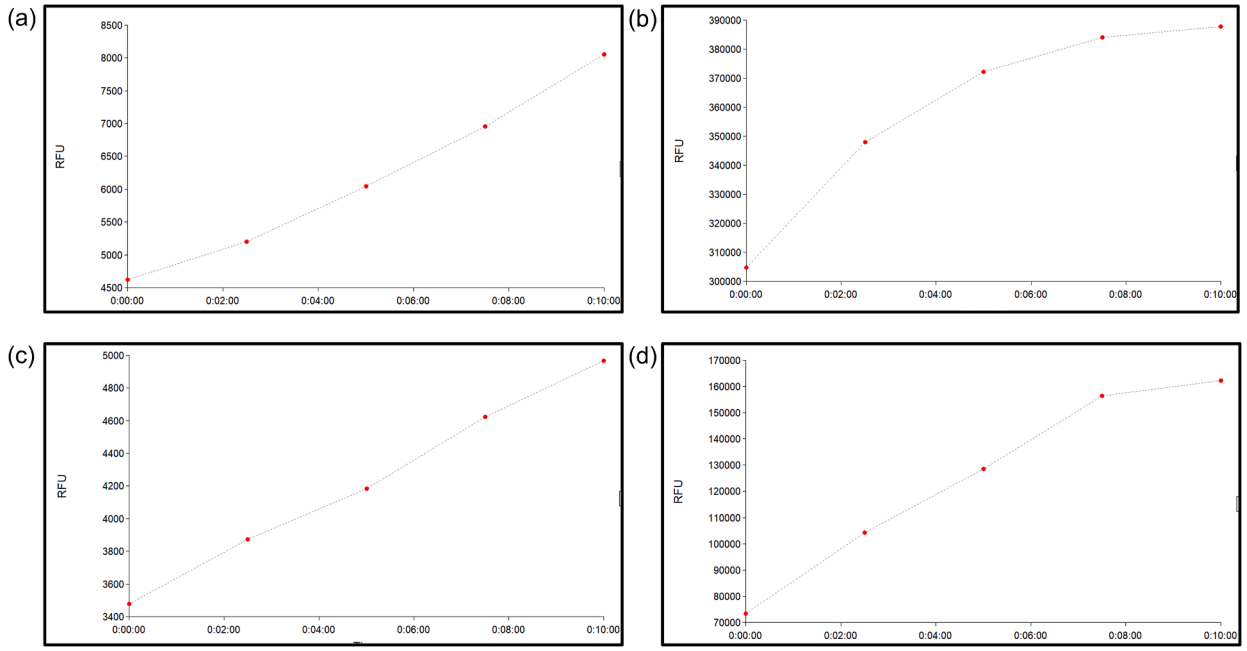

Fig. 3. Raw fluorescence (Y-axis) shown as a function of time (X-axis in minutes) from representative samples processed on a standard multimode plate reader. (a) N – gene target not detected in this clinical specimen whereas (b) a prominent spike in fluorescence is noted from a separate clinical sample in which the N – gene target is robustly detected (note RFU is an order of magnitude greater on Y-axis compared to panel 'a'). A similar pattern is shown in the bottom two panels where the *ORF1ab* target is not detected (panel c) versus detected (panel d). Similarly, the Y-axis values are an order of magnitude higher between the two scenarios (e.g. detected/not detected) due to the collateral activity of the CRISPR Cas13 guide RNAs to cleave and release fluorescence in the presence of SARS-CoV-2.

other viral diseases besides COVID-19 [17]. Similarly, SHERLOCK methods have exploited CRISPR-mediated detection of SARS-CoV-2 with comparable sensitivity to RT-PCR[18]. These tests, and earlier versions of this technology, have rapidly detected nuclei acids in human health applications[10]. The SHERLOCK approach, in particular, has been compatible not only with fluorescence read outputs but also lateral-flow assays[10,18]. Moreover, flexibility in constructing CRISPR RNAs and other RNA sequences continue to push the detection limit and turnaround time for CRISPR diagnostics. Of note, a limit of detection of 12 copies/μL and a 45 min run time has been reported for SARS-CoV-2 RNA detection using the Cas12 system[19]. This assay, termed DETECTR was given EUA status, and examines the N2 portion of the N gene. The Sherlock CRISPR SARS-CoV-2 kit corroborates these findings and expands the repertoire of viral genomic analyses to the Cas13 CRISPR-Cas effector family using fluorescence-based detection. By contrast to the DETECTR assay, the SHERLOCK approach used in the current study examined two SARS-CoV-2 gene targets (N and ORF1ab). Overall Sherlock's CRISPR SARS-CoV-2 kit exhibited a limit of detection down to 6.75 copies/μL, as mentioned above, and had an approximate process time of 50 min.

As advances in COVID-19 diagnostics emerge, CRISPR testing, because of its many advantages, will be at the forefront. [12,16]. This is further underscored by the 2020 Nobel prize awarded towards this disruptive technology[20,21]. In the context of the current work, SHERLOCK technology is also poised to rapidly detect SARS-CoV-2 RNA from other sample matrices e.g. saliva).

The COVID-19 pandemic has accelerated CRISPR diagnostics and we are only at the beginning of this revolution. One of the unique features of the SHERLOCK approach applied here is that viral RNA can be directly detected with high accuracy and the CRISPR-Cas13 enzyme is rapidly programmable to detect any RNA based target. Further, the reaction time has a brief LAMP step (under 30 min) and the detection process is an order of magnitude faster from loading the 384-well plate into the plate reader to result output (10 min). This is currently not possible with other RT-PCR amplification-based methods. From a public health and governance perspective, the development of fast, accurate and a portable point of care diagnostic tests is critical for imminent infectious diseases outbreaks and surveillance[22;23]. A test such as the one deployed in our clinical setting will be indispensable in the current stage of the pandemic as it does not require large equipment and obviates the need for in-demand PCR consumables.

5. Author contributions statement

G.J.T. and W.A.K contributed to study concept and design. R.E.B and W.A.K. contributed to experiment set-up, data acquisition, and analysis. All authors contributed to interpretation of data and critical review of the manuscript.

Declaration of Competing Interest

The authors declare no competing interests.

Acknowledgements

We thank members of SHERLOCK Biosciences for sharing reagents, initial EUA data, and valuable feedback for this project. The authors acknowledge the support of the Laboratory for Clinical Genomics and Advanced Technology in the Department of Pathology and Laboratory Medicine of the Dartmouth Hitchcock Health System.

References

[1] E. Dong, H. Du, L. Gardner, An interactive web-based dashboard to track COVID-19 in real time, Lancet Infect. Dis. 20 (2020) 533–534.
[2] C. Huang, et al., Clinical features of patients infected with 2019 novel coronavirus in Wuhan, China. Lancet 395 (2020) 497–506.
[3] C. Wang, P.W. Horby, F.G. Hayden, G.F. Gao, A novel coronavirus outbreak of global health concern, Lancet 395 (2020) 470–473.
[4] N. Zhu, et al., A Novel Coronavirus from Patients with Pneumonia in China, N. Engl. J. Med. 382 (2019) 727–733, 2020.
[5] Y. Bai, et al., Presumed asymptomatic carrier transmission of COVID-19, JAMA 323 (2020) 1406–1407.
[6] A. Kimball, et al., Asymptomatic and presymptomatic SARS-CoV-2 infections in residents of a long-term care skilled nursing facility - king county, March 2020, MMWR Morb Mortal Wkly Rep 69 (2020) 377–381.
[7] O.O. Abudayyeh, et al., C2c2 is a single-component programmable RNA-guided RNA-targeting CRISPR effector, Science 353 (2016) aaf5573.
[8] Y. Ishino, M. Krupovic, P. Forterre, History of CRISPR-cas from encounter with a mysterious repeated sequence to genome editing technology, J. Bacteriol. (2018) 200.
[9] J.S. Gootenberg, et al., Nucleic acid detection with CRISPR-Cas13a/C2c2, Science 356 (2017) 438–442.
[10] C. Myhrvold, et al., Field-deployable viral diagnostics using CRISPR-Cas13, Science 360 (2018) 444–448.
[11] T. Hou, et al., Development and evaluation of a rapid CRISPR-based diagnostic for COVID-19, PLoS Pathog. 16 (2020), e1008705.
[12] M.J. Kellner, J.G. Koob, J.S. Gootenberg, O.O. Abudayyeh, F. Zhang, SHERLOCK: nucleic acid detection with CRISPR nucleases, Nat. Protoc. 14 (2019) 2986–3012.
[13] T. Notomi, et al., Loop-mediated isothermal amplification of DNA, Nucleic Acids Res. 28 (2000) E63.
[14] J.A. Lefferts, E.J. Gutmann, I.W. Martin, W.A. Wells, G.J. Tsongalis, Implementation of an Emergency use authorization test during an impending national crisis, J. Mol. Diagn. 22 (2020) 844–846.
[15] J.A. Tweed, et al., Automated sample preparation for regulated bioanalysis: an integrated multiple assay extraction platform using robotic liquid handling, Bioanalysis 2 (2010) 1023–1040.
[16] M.N. Esbin, et al., Overcoming the bottleneck to widespread testing: a rapid review of nucleic acid testing approaches for COVID-19 detection, RNA 26 (2020) 771–783.
[17] J.S. Chen, et al., CRISPR-Cas12a target binding unleashes indiscriminate single-stranded DNase activity, Science 360 (2018) 436–439.
[18] J. Joung, et al., Detection of SARS-CoV-2 with SHERLOCK One-Pot Testing, N. Engl. J. Med. 383 (2020) 1492–1494.
[19] J.P. Broughton, et al., CRISPR-Cas12-based detection of SARS-CoV-2, Nat. Biotechnol. 38 (2020) 870–874.
[20] P. Patsali, M. Kleanthous, C.W. Lederer, Disruptive Technology: cRISPR/Cas-Based Tools and Approaches, Mol. Diagn. Ther. 23 (2019) 187–200.
[21] Chemistry Nobel Honors CRISPR, an 'Essential' Tool for Cancer, Cancer Discov. (2020), https://doi.org/10.1158/2159-8290.CD-NB2020-090.
[22] L.H. Nguyen, et al., Risk of COVID-19 among front-line health-care workers and the general community: a prospective cohort study, Lancet Public Health 5 (2020) e475–e483.
[23] X. Xiang, et al., CRISPR-cas systems based molecular diagnostic tool for infectious diseases and emerging 2019 novel coronavirus (COVID-19) pneumonia, J. Drug Target 28 (2020) 727–731.